



## **Optical Band gap characterization of Novel Nanoscale CBM- CZF composite**

**Allwin Sudhakaran, Ashwin Sudhakaran, E. Siva Senthil\***

Department of Physics, Karpagam Academy of Higher Education, Coimbatore, Tamilnadu, India

\*Corresponding Author: [sivasenthil.e@kahedu.edu.in](mailto:sivasenthil.e@kahedu.edu.in)

### **ABSTRACT**

*The present study is aimed mainly on optical property of novel copper doped barium hexaferrite (CBM)-cobalt zinc ferrite (CZF) composite prepared by physical mixing technique. The structural analysis from XRD results showed successful formation of spinel and hexagonal ferrites which matched very well with the JCPDS card data. The morphological analysis from SEM image verified the spherical microstructure with uniform distribution. The structural, morphological and optical parameters were greatly affected by the concentration of CBM in composite. The optical bandgap was measured using Tauc's plot which showed a maximum value of 2.84eV for CBM-CZF 80-20. These environmentally friendly biocompatible magnetic composites can be used for optoelectronic, medical and other health science applications including major and minor load-bearing implants, nano-contrast MR imaging agents for MRI systems, and wide bandgap semiconductors.*

**Keywords:** copper doped barium, hexaferrite, cobalt doped zinc Ferrite, sol-gel citrate, physical mixing, Tauc's Plot.

Received 11.03.2022

Revised 16.03.2022

Accepted 02.04.2022

### **INTRODUCTION**

Nanoparticles and nanocomposites have attracted significant interest in various fields such as biology, medicine, electronics and chemistry in recent years. Polymer/metal nanocomposites consisting of polymer as matrix and metal nanoparticles as nanofiller commonly show several attractive advantages such as electrical, mechanical, biomedical related healthcare features. The polymer/metal nanocomposites for biomedical applications are extensively studied in several categories including strong and stable materials, conductive devices, sensors and biomedical products. The usage of ferrites in various fields have attained a major interest all over the world [1]. Composites are made by joining two ferrite materials with different geometry (0-3, 1-3, 2-2) using proper synthesis method [2]. One among them (0-3 type composites) have a greater benefit due to its low synthesis cost and faster reaction time [3]. Scientists from all over the world were trying to enhance the properties of such composite materials [4]- [7]. Generally doping copper in barium hexaferrite helps in increasing the coercivity which can be used for magnetic storage media. It is found that just 0 to 8 percentage of copper increases the coercivity up to 851-856 Oe, where the saturation magnetization is increased from 11 to 34 emu/g [8]. The magnetic properties of copper doped barium hexaferrite shows irregularity at  $x=1$  which aligns well within the crystal structure. However, this is not in the case of electrical properties, as the size of the copper ions are much greater it finds difficult to enter into the Fe lattice of barium hexaferrite for  $x \geq 1$  [9]. On the other hand, increasing the concentration of Zinc ions replaces the cobalt ions resulting in high coercivity value in cobalt zinc ferrite [10]. Lately the magnetic interactions between Barium hexaferrite with cobalt zinc ferrite composite have been studied in detail which revealed much understanding over its magnetic properties [11]-[13]. The present composite material under study is copper doped barium hexaferrite (CBM)- Cobalt zinc ferrite (CZF). The hard site (CBM) and soft site (CZF) were synthesized by citrate sol-gel method separately and later made into composite using physical mixing technique. The composite was made with different hard to soft ratio such as 90% CBM with 10% CZF (HS90-10) and 80% CBM with 20% CZF (HS80-20) respectively  $[(\text{CuBaFe}_{12}\text{O}_{19})_{1-x}/(\text{CoZnFe}_2\text{O}_4)_x]$  and are annealed at 800°C for 3 hours.

## MATERIAL AND METHODS

### Preparation and Synthesis of CBM

Citrate sol-gel method was followed to synthesize nanocopper doped barium hexaferrite (CBM). The precursors, nitrates of copper, barium and iron were mixed with citric acid in deionized water at 1:2 ratio in magnetic stirrer for 1 hour. The pH of 7 was maintained by adding ammonia solution. The solution is then heated in a hotplate until a dried powder is obtained. This powder was later grounded with mortar and pestle and kept at furnace at 850 °C for 2 hours to get the final CBM nanoparticles[14].

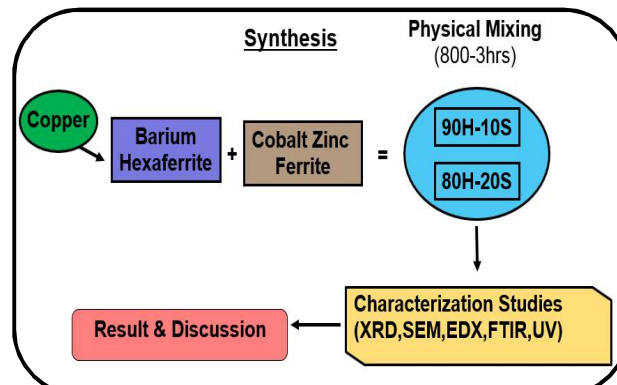


Figure 1. Research outline.

### Synthesis of CZF

Sol-gel citrate method is carried out for the preparation of cobalt doped zinc ferrite. Here the nitrates of zinc, iron and cobalt are taken in a beaker containing deionized water and mixed with citric acid at 1:1 ratio in magnetic stirrer at 1000 RPM for 1 hour. Temperature of the magnetic stirrer was increased gradually until the solution turns into a viscous gel. Later at certain temperature the gel converts into a dry powder which was grounded and kept inside muffle furnace at 800 °C for 5 h to get nano CZF particles[15].

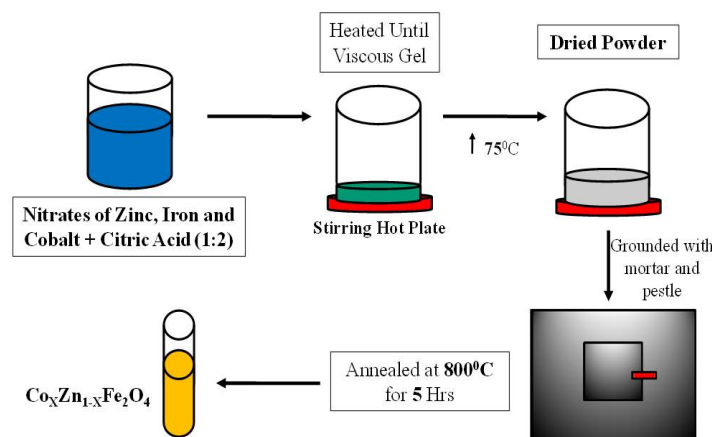
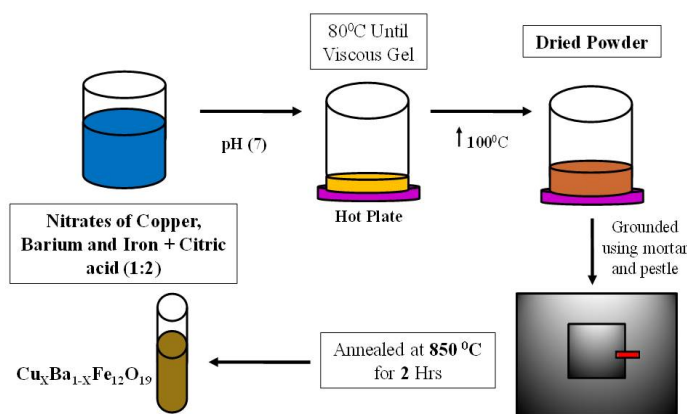


Figure 3. Preparation of CZF by Sol-gel citrate technique.

### Synthesis of nano CBM-CZF composite

Physical mixing route is carried out for the preparation of CBM-CZF composite method [16], [17]. Here the ratio of CBM-CZF are taken as 90-10 and 80-20 respectively  $[(\text{Cu}_{0.5}\text{Ba}_{0.5}\text{Fe}_{12}\text{O}_{19})_{1-x}/(\text{Co}_{0.6}\text{Zn}_{0.4}\text{Fe}_2\text{O}_4)_x]$  which are denoted as HS90-10 and HS80-20 respectively. The mixed powders are grounded well physically for 1 hour with the help of mortar and pestle and kept at 800°C for 3 h in air atmosphere before sending them for characteristic studies.



**Figure 2.** Preparation of CBM by citrate Sol-gel technique.

### EXPERIMENTAL TECHNIQUES

3<sup>rd</sup> generation Empyrean XRD (Malvern Panalytical) with 1.540 copper K alpha radiation is used to measure the structural parameters of the prepared composite material. The M-type Hexagonal and Spinel ferrite formations within the composite were confirmed using Shimadzu FTIR(IR affinity 1A) spectra recorded within 4000-400 cm<sup>-1</sup> range. The morphology and the size of the composite particles were analyzed using SEM image (Jeol JSM 6390 model) EDX was carried out to determine the elemental composition. UV 2400PC Series with 360nm light source and 1nm slit width is used to measure the optical bandgap of the composite material within 800-200nm range

### RESULTS AND DISCUSSION

#### Structural studies

The structural parameters of the composite were studied using XRD which matched with the JCPDS card data 78-0133 for CBM and 88-2152 for CZF respectively confirming the hexagonal (P63/mmc space group for CBM) and cubic (Fd-3m space group for CZF) structures. The lattice parameter and cell volume were measured and tabulated as shown below (table 1).

With the help of Scherrer's equation the average size of the composite were measured using the peaks (106), (1011), (116), (108), (109), (118) as tabulated below (table 2). From the table it is clear that the average size increases with the increase in CBM concentration.

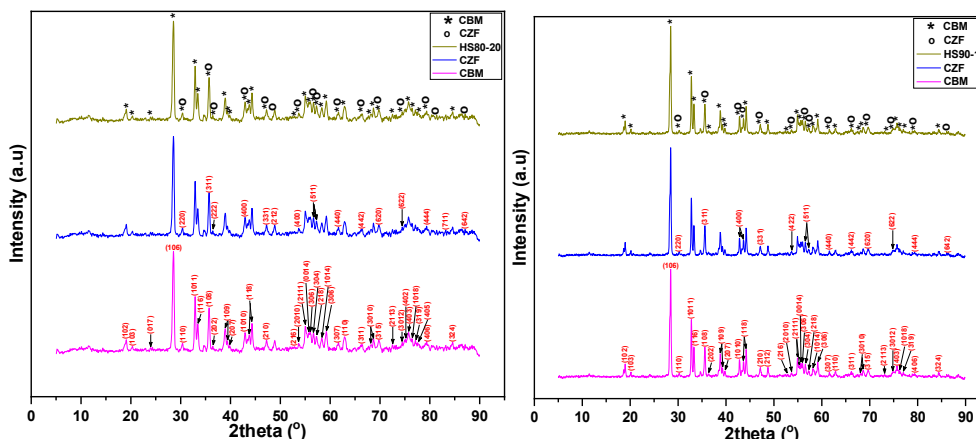


**Figure 4.** XRD peaks of (a) HS90-10 and (b) HS80-20 respectively.

#### Morphology studies

From the SEM image the distribution of particle size was calculated using ImageJ software (figure 5). The image reveals uniform distribution of spherical micro structured particle in which single particle agglomerate to form grains separated by grain boundaries resulting in greater grain size (measured using SEM image) than crystalline size (measured using XRD)[18].

The chemical composition over the prepared composite material were studied using EDAX analysis (figure 6). The results from EDAX confirmed the purity of the prepared sample as tabulated below (table 3).

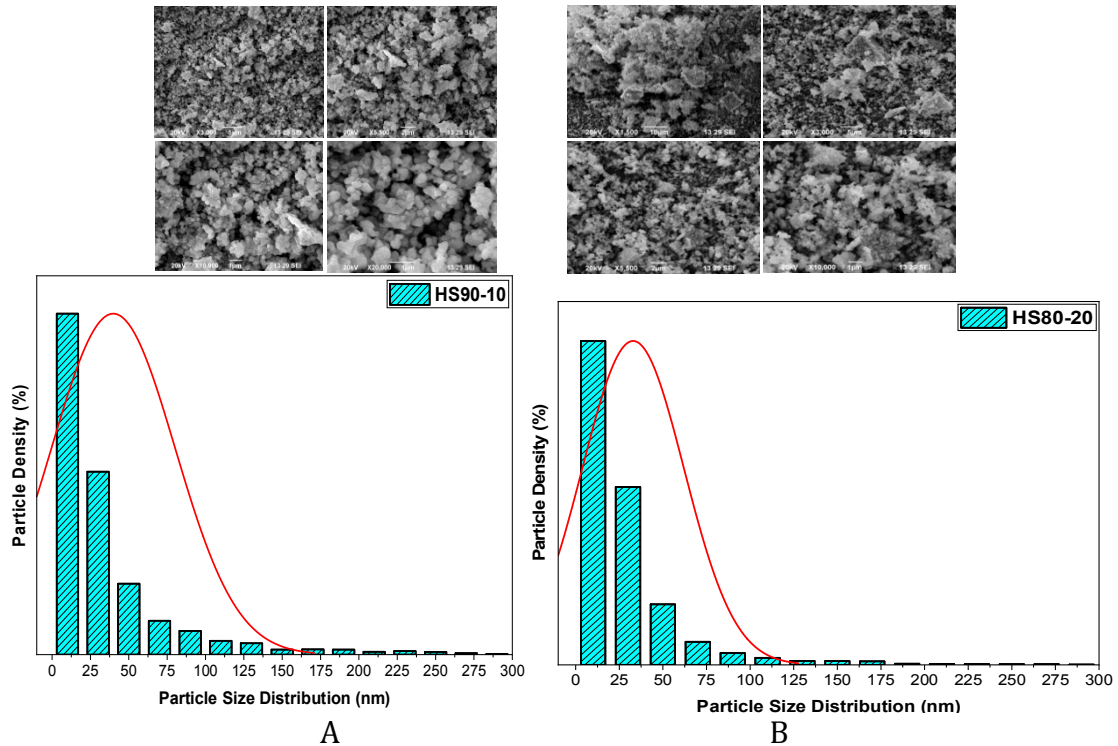


Figure 5. SEM image with histogram of (a) HS90-10 and (b) HS80-20 samples.

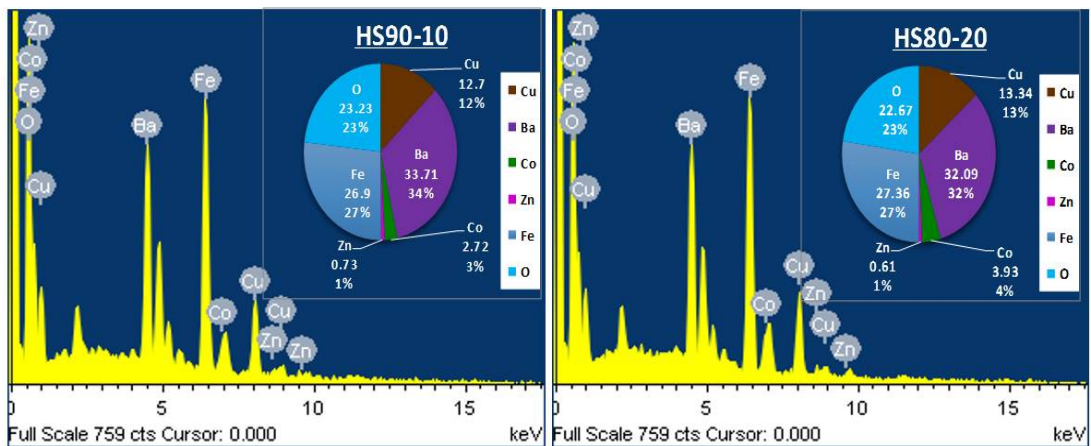


Figure 6. EDX results of CBM-CZF composite.

### FTIR Studies

The FTIR studies of CBM-CZF composite revealed the presence of  $V_1$ ,  $V_2$ , and  $V_3$  bands. The band  $V_1$  ( $538-605\text{cm}^{-1}$ ) represents the stretching complexes of  $\text{Zn}^{2+}$  ions in tetrahedral metal-oxygen bond. The band  $V_2$  ( $410-470\text{cm}^{-1}$ ) represents the octahedral complexes confirming the formation of Iron-oxygen bond within the composite material. The band  $V_3$  corresponds to the characteristic peak of iron-oxygen bond. The bands 551 and 569 represent the characteristic peaks of cobalt ferrite. The O-H bending at 1635 represents that the M-type Hexaferrite nanoparticles are formed successfully.

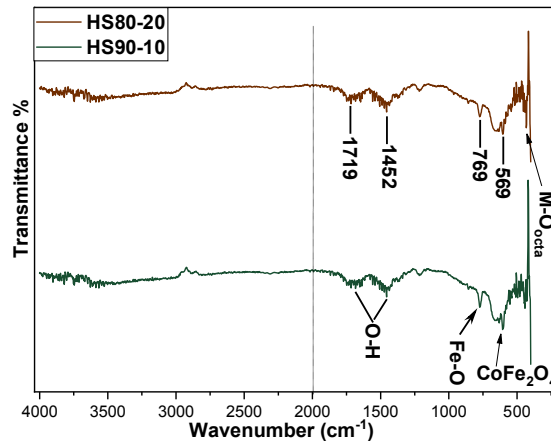


Figure 7. FTIR result of HS90-10 and HS80-20 sample

### Optical Bandgap Studies

Using UV spectroscopy, the optical bandgap of the prepared composite material was calculated. From the Tauc's plot the optical bandgap energy was found to be 2.65eV for HS90-10 which is much lesser when compared to HS80-20 (2.8456eV) sample. This confirms that the concentration of CBM greatly affects the optical properties of the prepared composite material which can be greatly useful for opto-electronic applications.

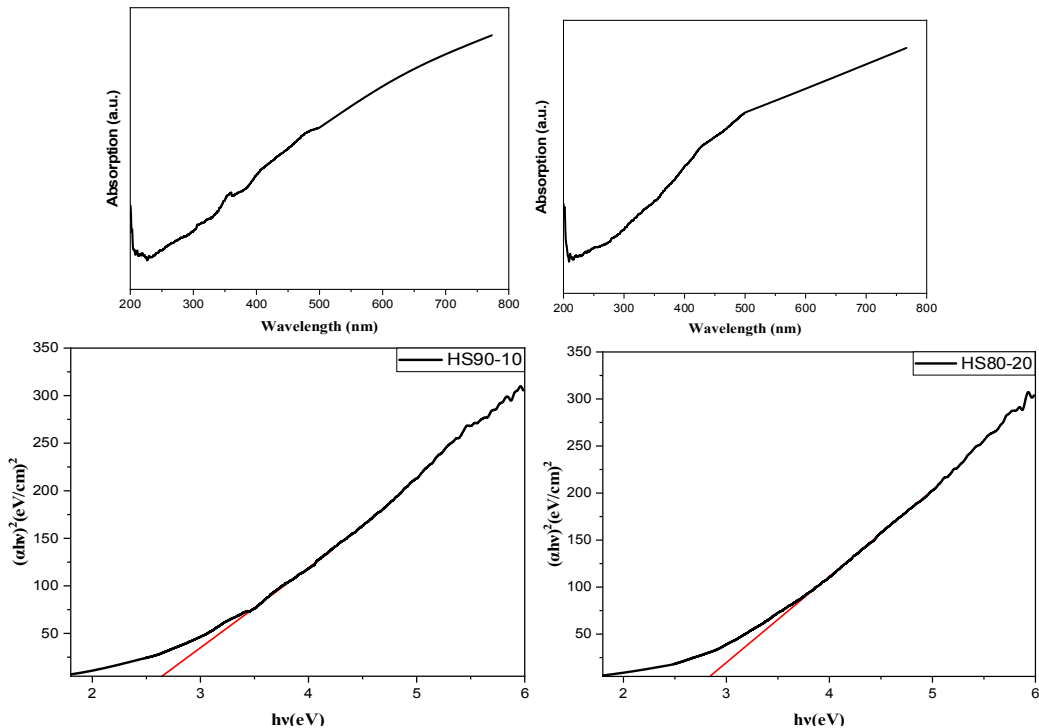


Figure 8. Tauc's plot with Absorption results for (a) HS90-10 and (b) HS80-20 respectively.

Table 1. calculated structural parameters of HS80-20 and HS90-10 samples.

	a	c	Cell Volume(V)
<b>Standard JCPDS value</b>			
<b>CBM: 78-0133</b>	5.865	23.099	688.113
<b>CZF: 88-2152</b>	8.396	=	591.858
<b>Calculated Value of HS80-20</b>			
<b>CBM(0014)</b>	-	23.0314	683.975
<b>CBM (210)</b>	5.856	-	
<b>CZF (311)</b>	8.303	=	572.443
<b>Calculated Value of HS90-10</b>			
<b>CBM(0014)</b>	-	23.066	688.271
<b>CBM(210)</b>	5.870	-	
<b>CZF (311)</b>	8.328	=	577.572

CBM-CZF	Peaks	Particles Range (nm)		Average size (nm)
		From	To	
HS80-20	(106), (1011), (116),	20.60	28.02	24.65
HS90-10	(108), (109), (118)	24.94	37.14	31.81

**Table 2.** Average size of CBM-CZF composite.

Sample	Chemicals present	HS90-10			HS80-20		
		Apparent Concentration	Weight %	Atomic %	Apparent Concentration	Weight %	Atomic %
CBM-CZF	Copper	4.48	12.70	8.20	4.70	13.34	8.65
	Barium	12.41	33.71	10.07	11.83	32.09	9.63
	Iron	9.84	26.90	19.77	10.04	27.36	20.19
	Oxygen	13.94	23.23	59.60	13.53	22.67	58.39
	Cobalt	1.00	2.72	1.90	1.45	3.93	2.75
	Zinc	0.26	0.73	0.46	0.22	0.61	0.38
<b>Total</b>		100.00			100.00		

**Table 3.** chemical composition of HS90-10 and HS80-20 measured using EDAX analysis

Absorption (cm <sup>-1</sup> )	Functional Group
V2 (410-470)	Fe-O Stretching confirming M-O <sub>octa</sub>
V1 (538-605)	M-O <sub>tetra</sub>
551, 569	Characteristic peak of CoFe <sub>2</sub> O <sub>4</sub>
V3 (630-773)	Characteristic peak of Fe-O
1400-1800	O-H Deformation, Evidence for M-Ferrite nanoparticles formation

**Table 4.** FTIR Tabulation for nano CBM-CZF composite.

## DISCUSSION

According to the author, these results are remarkable and unique. The composite is naturally a biocompatible magnetic material possessing soft ferromagnetic or super paramagnetic behavior based on its particle size and temperature. Such materials can be used as nano-contrast MR imaging agents for MRI systems and other health science applications [19]. Also, all materials in the composite are non-toxic to human tissues and thus can be modified to make major load-bearing implants having less stiffness and performance closer to human bone or minor implants including screws, pins, and plates [20, 21]. Due to their wider semiconducting bandgap, they can be greatly utilized for optoelectronic applications. These hexaferrites, as magnetic materials, are attractive candidates for health science and biomedical applications for diagnosis, therapeutics, control and treatment of diseases, enhanced MRI imaging, magnetic hyperthermia cancer treatment, targeted drug and gene delivery, biolabeling, biosensing, and antimicrobial agents, and enable the development of new medical devices. Using ferrites as nanoprobe to label biomolecules offers the advantage of robust signal strength, sensitivity, and stability. Ferrite nanoparticles can be functionalized with different ligands to provide affinity for specific biological analytes to bind to the targeted surfaces, e.g., specific tumor types. Since the principle constituents of many ferrites, such as Fe, Mn, and Zn, exist as required metabolic minerals in the body, toxicity is rarely a limiting factor, unlike, for example, gadolinium-based MRI contrast agents.

## CONCLUSION

Thus, physical mixing technique was carried out to synthesize novel copper doped barium hexaferrite-cobalt zinc ferrite composite successfully. From the results it is clear that the concentration of CBM with CZF greatly affects the characteristic behavior of the material. The structural parameters obtained from XRD matched well with JCPDS data which revealed effective formation of both CBM and CZF nanoparticles within the composite. The results also showed that the concentration of CBM and CZF greatly affects the lattice parameter, cell volume and average size of the composite. From SEM image it is clear that the composite have good crystalline structure with spherical microstructure and uniform distribution of grain size. The EDAX further confirmed the purity within the composite. The formation of metal-oxygen bond for spinel ferrite as well as M-type hexaferrite were confirmed using FTIR studies. From Tauc's plot the optical bandgap energy was measured which is maximum for HS80-20 (2.84 eV) sample.

**DECLARATION OF COMPETING INTEREST**

The authors declare that they have no known competing financial interests or personal relationships that could have appeared to influence the work reported in this paper.

**ACKNOWLEDGEMENT**

We, the authors are thankful to our President, Chancellor, Chief Executive Officer, Vice Chancellor and Registrar of Karpagam Academy of Higher Education, Coimbatore, India for providing facilities and encouragement. Our thanks are also due to Sophisticated Analytical Instrument Facility (SAIF) for VSM Analysis.

**REFERENCES**

1. S. D. Bader, (2006). "Colloquium: Opportunities in nanomagnetism," *Reviews of Modern Physics*, vol. 78, no. 1, doi: 10.1103/RevModPhys.78.1.
2. Y. Wang, J. Hu, Y. Lin, and C. W. Nan, (2010)., "Multiferroic magnetoelectric composite nanostructures," *NPG Asia Materials*, vol. 2, no. 2. pp. 61–68. doi: 10.1038/asiamat.2010.32.
3. R. Kumar, S. Guha, R. K. Singh, and M. Kar, (2018). "Surface anisotropy induced magnetism in BaTiO<sub>3</sub>-CoFe<sub>2</sub>O<sub>4</sub> (BTO-CFO) nanocomposite," *Journal of Magnetism and Magnetic Materials*, vol. 465, pp. 93–99, doi: 10.1016/j.jmmm.2018.05.061.
4. D. T. M. Hue *et al.*, (2013). "Synthesis, structure, and magnetic properties of SrFe<sub>12</sub>O<sub>19</sub>/La<sub>1-x</sub>CaxMnO<sub>3</sub> hard/soft phase composites," *Journal of Applied Physics*, vol. 114, no. 12, Sep. doi: 10.1063/1.4821971.
5. N. A. Algarou *et al.*, (2020). "Magnetic and microwave properties of SrFe<sub>12</sub>O<sub>19</sub>/MCo<sub>0.04</sub>Fe<sub>1.96</sub>O<sub>4</sub> (M = Cu, Ni, Mn, Co and Zn) hard/soft nanocomposites," *Journal of Materials Research and Technology*, vol. 9, no. 3, pp. 5858–5870. doi: 10.1016/j.jmrt.2020.03.113.
6. A. Quesada, F. Rubio-Marcos, J. F. Marco, F. J. Mompean, M. García-Hernández, and J. F. Fernández, (2014). "On the origin of remanence enhancement in exchange-uncoupled CoFe<sub>2</sub>O<sub>4</sub>-based composites," *Applied Physics Letters*, vol. 105, no. 20, doi: 10.1063/1.4902351.
7. K. Raidongia, A. Nag, A. Sundaresan, and C. N. R. Rao, (2010). "Multiferroic and magnetoelectric properties of core-shell CoFe<sub>2</sub>O<sub>4</sub>@BaTiO<sub>3</sub> nanocomposites," *Applied Physics Letters*, vol. 97, no. 6, doi: 10.1063/1.3478231.
8. S. Vadivelan and N. Victor Jaya, (2016). "Investigation of magnetic and structural properties of copper substituted barium ferrite powder particles via co-precipitation method," *Results in Physics*, vol. 6, pp. 843–850, doi: 10.1016/j.rinp.2016.07.013.
9. S. Kumar, S. Guha, S. Supriya, L. K. Pradhan, and M. Kar, (2020). "Correlation between crystal structure parameters with magnetic and dielectric parameters of Cu-doped barium hexaferrite," *Journal of Magnetism and Magnetic Materials*, vol. 499, doi: 10.1016/j.jmmm.2019.166213.
10. R. C. Alange and R. C. Alange, (2021). "Structural and Magnetic Properties of Zn<sup>2+</sup> Doped Cobalt Ferrite Nanoparticles Synthesized by Sol-gel Auto Combustion Method Structural and Magnetic Properties of Zn<sup>2+</sup> Doped Cobalt Ferrite Nanoparticles Synthesized by Sol-gel Auto Combustion Method," *Article in International Journal of Science and Research*, doi: 10.21275/SR21719065226.
11. M. K. Manglam, J. Mallick, S. Kumari, R. Pandey, and M. Kar, (2021). "Crystal structure and magnetic properties study on barium hexaferrite (BHF) and cobalt zinc ferrite (CZF) in composites," *Solid State Sciences*, vol. 113, doi: 10.1016/j.solidstatesciences.2020.106529.
12. M. K. Manglam, S. Kumari, S. Guha, S. Datta, and M. Kar, (2020). "Study of magnetic interaction between hard and soft magnetic ferrite in the nanocomposite," in *3RD INTERNATIONAL CONFERENCE ON CONDENSED MATTER AND APPLIED PHYSICS (ICC-2019)*, vol. 2220, p. 110020. doi: 10.1063/5.0001220.
13. J. Mallick, M. K. Manglam, S. Datta, and M. Kar, (2020). "Evidence of magnetic interaction between BaFe<sub>12</sub>O<sub>19</sub> and CuFe<sub>2</sub>O<sub>4</sub> in the nanocomposite," in *3RD INTERNATIONAL CONFERENCE ON CONDENSED MATTER AND APPLIED PHYSICS (ICC-2019)*, vol. 2220, p. 110025. doi: 10.1063/5.0001223.
14. S. Kumar, S. Guha, S. Supriya, L. K. Pradhan, and M. Kar, (2020). "Correlation between crystal structure parameters with magnetic and dielectric parameters of Cu-doped barium hexaferrite," *Journal of Magnetism and Magnetic Materials*, vol. 499, p. 166213, doi: 10.1016/j.jmmm.2019.166213.
15. J. Feng, R. Xiong, Y. Liu, F. Su, and X. Zhang, (2018). "Preparation of cobalt substituted zinc ferrite nanopowders via auto-combustion route: an investigation to their structural and magnetic properties," *Journal of Materials Science: Materials in Electronics*, vol. 29, no. 21, pp. 18358–18371. doi: 10.1007/s10854-018-9950-y.
16. J. D. Bobić *et al.*, (2018). "PZT-nickel ferrite and PZT-cobalt ferrite comparative study: Structural, dielectric, ferroelectric and magnetic properties of composite ceramics," *Ceramics International*, vol. 44, no. 6, pp. 6551–6557. doi: 10.1016/j.ceramint.2018.01.057.
17. A. Alipour, S. Torkian, A. Ghasemi, M. Tavoosi, and G. R. Gordani, (2021). "Magnetic properties improvement through exchange-coupling in hard/soft SrFe<sub>12</sub>O<sub>19</sub>/Co nanocomposite," *Ceramics International*, vol. 47, no. 2, pp. 2463–2470, doi: 10.1016/j.ceramint.2020.09.089.
18. S. Kumar, S. Supriya, L. K. Pradhan, and M. Kar, (2017). "Effect of microstructure on electrical properties of Li and Cr substituted nickel oxide," *Journal of Materials Science: Materials in Electronics*, vol. 28, no. 22, pp. 16679–16688, doi: 10.1007/s10854-017-7580-4.
19. Ghasemian, Z., Shahbazi-Gahrouei, D., & Manouchehri, S. (2015). "Cobalt Zinc Ferrite Nanoparticles as a Potential Magnetic Resonance Imaging Agent: An In vitro Study," *Avicenna journal of medical biotechnology*, 7(2), 64–68.



20. Kannan, M.B., Moore, C., Saptarshi, S. et al. (2017). "Biocompatibility and biodegradation studies of a commercial zinc alloy for temporary mini-implant applications", *Sci Rep* 7, 15605. <https://doi.org/10.1038/s41598-017-15873-w>.
21. T. Charoensuk, W. Thongsamrit, C. Ruttanapun, P. Jantaratana, C. Sirisathitkul, (2021). "Loading Effect of Sol-Gel Derived Barium Hexaferrite on Magnetic Polymer Composites", *Nanomaterials*, Vol. 11, p. 558. DOI: <https://doi.org/10.3390/nano11030558>.

#### CITATION OF THIS ARTICLE

A Sudhakaran, A Sudhakaran, E. Siva Senthil. Optical Band gap characterization of Novel Nanoscale CBM- CZF composite. *Bull. Env.Pharmacol. Life Sci.*, Spl Issue [1] 2022 : 643-650